THE JOURNAL OF BIOLOGICAL CHEMISTRY
Vol. 275, No. 50, Issue of December 15, pp. 39213–39222, 2000

Printed in U.S.A.

Processing and Sorting of the Prohormone Convertase 2 Propeptide*

Received for publication, April 26, 2000, and in revised form, August 22, 2000
Published, JBC Papers in Press, September 19, 2000, DOI 10.1074/jbc.M003547200

Laurent Muller‡§, Angus Cameron‡, Yolanda Fortenberry¶, Ekaterina V. Apletalina, and Iris Lindberg‡‖

From the Department of Biochemistry and Molecular Biology, LSU Health Sciences Center, New Orleans, Louisiana 70112

The prohormone convertases (PCs) are synthesized as zymogens whose propeptides contain several multibasic sites. In this study, we investigated the processing of the PC2 propeptide and its function in the regulation of PC2 activity. By using purified pro-PC2 and directed mutagenesis, we found that the propeptide is first cleaved at the multibasic site separating it from the catalytic domain (primary cleavage site); the intact propeptide thus generated is then sequentially processed at two internal sites. Unlike the mechanism described for furin, our mutagenesis studies show that internal cleavage of the propeptide is not required for activation of pro-PC2. In addition, we identified a point mutation in the primary cleavage site that does not prevent the folding nor the processing of the zymogen but nevertheless results in the generation of an inactive PC2 species. These data suggest that the propeptide cleavage site is directly involved in the folding of the catalytic site. By using synthetic peptides, we found that a PC2 propeptide fragment inhibits PC2 activity, and we identified the inhibitory site as the peptide sequence containing basic residues at the extreme carboxyl terminus of the primary cleavage site. Finally, our study supplies information concerning the intracellular fate of a convertase propeptide by providing evidence that the PC2 propeptide is generated and is internally processed within the secretory granules. In agreement with this localization, an internally cleaved propeptide fragment could be released by stimulated secretion.

A feature common to a great variety of secreted and membrane proteins, ranging from receptors to peptide hormones and neuropeptides, is initial synthesis as a precursor that must undergo endoproteolytic processing in order to acquire biological activity (for reviews see Refs. 1 and 2). A family of mammalian serine proteases responsible for these proteolytic maturation events, termed the prohormone/proprotein convertases (PCs),[1] has been identified in the last 10 years (for reviews see Refs. 2–4). The PCs are structurally homologous to subtilisin and kexin and belong to the enzymatic superfamily of subtilases. All of the PCs contain the following five domains: an amino-terminal signal peptide that directs them to the secretory pathway; a propeptide of approximately 80–100 residues; a catalytic domain and a P domain, which are well conserved between PCs; and a carboxyl-terminal domain (which is specific for each PC). The P domain, only present within the eukaryotic subtilisin-like enzymes, is apparently required for activation (5) and may be responsible for regulation of enzymatic activity (6). The carboxyl-terminal domain is not required for activation but contains structural determinants necessary for the membrane attachment and the sorting of the PCs (7–10). Finally, the role of the propeptide remains to be determined precisely. This domain is specifically required for the activation of the PCs, and its proteolytic processing constitutes part of the mechanism of activation (7, 11, 12).

Propeptides have historically been involved in several different aspects of the post-translational modification and maturation of proproteins, both in the intracellular targeting, stabilization, and activation of proenzymes, as well as inhibition of their cognate enzymes. Propeptides are responsible for the targeting of cytosolic proteins (13) and secreted proteins, including proteases (14–16) and peptide precursors such as prosomatostatin (17, 18). Propeptides are also responsible for the stabilization of proenzymes, as in the case of cathepsins (19). Another major function of propeptides is their role in the activation of the mature protein they will form (20, 21). In the case of proteases, propeptides are involved in both the activation of the zymogen and the regulation of the activity of the mature enzyme (for review see Ref. 22). These features result both from the role of the propeptide as an intramolecular chaperone that controls zymogen folding and from the inhibitory potency of the propeptide. The intramolecular chaperone function of the propeptide was first demonstrated for prosubtilisin and pro-α-lytic protease and has since been extended to a number of proproteins (for reviews see Refs. 23–25).

Among these various functions, little is known concerning the role of the PC propeptides, because the activation mechanism of these zymogens has not yet been completely elucidated.

* This work was supported in part by National Institutes of Health Grants DK49703 and DA05084. The costs of publication of this article were defrayed in part by the payment of page charges. This article must therefore be hereby marked "*advertisement*" in accordance with 18 U.S.C. Section 1734 solely to indicate this fact.

‡ Both authors contributed equally to this work.

§ Present address: INSERM U36, Collège de France, 75231 Paris, France.

¶ Supported by National Institutes of Health Predoctoral Training Grant DK49703S2.

‖ Supported by a National Institute on Drug Abuse Research Scientist Development award. To whom correspondence should be addressed: Dept. of Biochemistry and Molecular Biology, LSU Health Sciences Center, 1901 Perdido St., New Orleans, LA 70112. Tel.: 504-568-4799; Fax: 504-568-6598; E-mail: ilindb@LSUHSC.edu.

[1] The abbreviations used are: PC, prohormone convertase; AMC, aminomethylcoumarin; α-MSH, α-melanocyte-stimulating hormone; ER, endoplasmic reticulum; TGN, trans-Golgi network; PMA, phorbol 12-myristate 13-acetate; RIA, radioimmunoassay; 7B2 CT, human 7B2-(155–186)-carboxy-terminal peptide; DMEM, Dulbecco's modified Eagle's medium; BSA, bovine serum albumin; HPLC, high pressure liquid chromatography; PAGE, polyacrylamide gel electrophoresis; Bis-Tris, 2-[bis(2-hydroxyethyl)amino]-2-(hydroxymethyl)propane-1,3-diol; MCA, methylcoumarinamide; ACTH, adrenocorticotropic hormone. CT peptide, carboxyl-terminal peptide of 7B2; CHO, Chinese hamster ovary.

The proposed model for the activation of the subtilases occurs through the following steps. 1) Autocatalytic cleavage of the propeptide; 2) binding of the propeptide to the mature enzyme, which results in inhibition of catalytic activity; and 3) inactivation/degradation of the propeptide, which terminates the inhibition by the propeptide (26). A study of the activation of furin provided evidence that this model could also be applicable to the PCs (27). Recently, the inhibitory potency of the PC1 and PC7 propeptides was also demonstrated (28, 29). Whereas the activation pathway of furin shares some characteristics with other PCs, the activation of PC2 is unique in the following respects (for review see Ref. 30). (i) The PC2 propeptide is not removed in the endoplasmic reticulum (ER) within minutes after synthesis but rather in the acidic compartments of the trans-Golgi network (TGN)/secretory granules with a half-life in the hour range (31–34). (ii) Intermediate molecular forms, including a major 71-kDa protein with an amino-terminally truncated propeptide, have been described in addition to pro-PC2 and PC2 (31, 33). (iii) Pro-PC2 must interact with the neuroendocrine protein 7B2 in the secretory pathway in order to become competent for activation (35); if 7B2 has not been encountered intracellularly, proteolytic removal of the propeptide leads to the formation of an inactive mature enzyme species, termed unproductive maturation (36, 37).

Pro-PC2 thus offers unique opportunities for delineating the role of the convertase propeptide in the activation mechanism of convertases. Indeed, pro-PC2 is the only PC that has been purified as an activable zymogen (38), thus permitting *in vitro* analysis of propeptide maturation. In addition, because pro-PC2 is the only PC that exits the ER as a zymogen, it is possible to distinguish between the following two steps in the folding process of its zymogen: global folding required for exit from the ER, and local folding of the catalytic site required for activation. Accordingly, we have been able to identify mutations in PC2 catalytic domain that result in the generation of proenzymes that are processed, in the TGN/secretory granules, into totally inactive PC2s (36).

In this report, we have investigated the following four aspects of the function of the propeptide in the activation of pro-PC2: 1) the processing of the propeptide *in vitro*, using purified recombinant pro-PC2; 2) the processing of the PC2 propeptide *in vivo*, using mutated pro-PC2s stably transfected in neuroendocrine cells; 3) the inhibitory potency of propeptide fragments using synthetic peptides; and 4) the fate of the propeptide in the TGN/secretory granules.

MATERIALS AND METHODS

Antisera—Unless specifically stated, all PC and peptide antisera used were polyclonal antisera raised in rabbits. The antiserum against PC2 (LSU18) was directed against a carboxyl-terminal peptide of mature PC2 (35). The antiserum against the PC2 propeptide (LSU26) was directed against residues His^{58}–Asp^{80} (Fig. 1, *hatched gray box*) of mouse pro-PC2 conjugated to keyhole limpet hemocyanin (Pierce) using 1-ethyl 3-(3-dimethylaminopropyl)carbodiimide; the peptide contained an amino-terminal tyrosine to enable iodination. The antiserum against α-melanocyte-stimulating hormone (α-MSH) was obtained from Chemicon (Temecula, CA) and was raised in sheep (39).

Cell Culture—AtT-20 cells were cultivated at 37 °C in 5% CO_2. AtT-20 cells were maintained in high glucose Dulbecco's modified Eagle's medium (DMEM) containing 10% Nuserum IV (Becton Dickinson, Franklin Lakes, NJ), and 2.5% fetal bovine serum (Irvine Scientific, Santa Ana, CA). Transfected cell lines were cultivated with either one or both of the following selection agents: 200 μg/ml active G418 (Life Technologies, Inc.) and/or 100 μg/ml hygromycin (Sigma). The AtT-20/PC2 cell line was kindly provided by Dr. R. E. Mains (The Johns Hopkins School of Medicine, Baltimore, MD) (34). We have already characterized the AtT-20/PC2/7B2 and the Rin/Proenkephalin/7B2 cell lines (40).

Site-directed Mutagenesis and Transfection—In order to obtain cell lines co-expressing 7B2 and mutated pro-PC2s, AtT-20 cells were first transfected with a pCEP4-derived plasmid (Invitrogen, Carlsbad, CA) encoding rat 27-kDa 7B2 (35). A high expressing clone was selected using immunoblotting and was supertransfected with pcDNA3 (Invitrogen) encoding mutated mouse pro-PC2 cDNAs. The mutations were obtained by the polymerase chain reaction-mediated primer overlap method as described previously (35). For this purpose a *Hin*dIII-*Kpn*I fragment of mouse pro-PC2 was amplified and reintroduced into the *Hin*dIII vector site and the pro-PC2 *Kpn*I site in *Hin*dIII/*Kpn*I-cut pcDNA3/pro-PC2. The mutagenesis primers used were as follows: 5′-GCCAAGCACAAGCACAGCCTACACCATAAGCGG-3′ and 5′-GCTGTGCTTGTGCTTGGCCTTTGCAAGCCCATT-3′ for the M53-56 mutant; 5′-GACAAGCACAAGCACGGGTACAGGGACATCAAT-3′ and 5′-CCCGTGCTTGTGCTTGTCAAATCCTTCTTGTTG-3′ for the M81-84 mutant; 5′-GTCCCTGTACCCGTGCTTTTTACGGTCAAATCC-3′ and 5′-AAGCACGGGTACAGGGACATCAAT-3′ for the R84H mutant; 5′-AAGGCAGGGTACAGGGACATCAAT-3′ and 5′-CCCTGCCTTTTTACGGTCAAATCC-3′ for the R84A mutant; and 5′-AAACACAGAGGGTACAGGGACATC-3′ and 5′-CCTGTACCCTCTGTGTTTACGGTCAAATCCTTC-3′ for the K83H mutant. All cDNA segments generated by polymerase chain reactions were verified by DNA sequencing. Cells were transfected using Lipofectin (Life Technologies, Inc.) (35). Three independent clones were analyzed for each mutation.

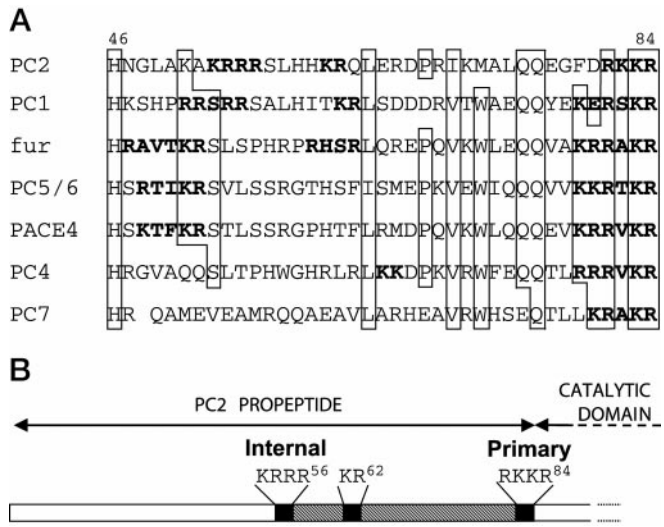

FIG. 1. **Structure of the PC propeptides.** *Panel A,* comparison of the propeptides of the 7 PCs. All sequences are from mouse except for rat PACE4. Residue numbers correspond to the mouse pro-PC2 sequence. Basic residues potentially involved in processing sites are in *bold*. Conserved residues are *boxed*. *Panel B,* cleavage sites within the pro-PC2 propeptide. *Closed boxes* correspond to the cleavage sites. The *hatched box* corresponds to the peptide used for immunization in the preparation of the propeptide antiserum LSU26. Numbering is taken from the sequence of mouse pro-PC2.

Metabolic Labeling and Immunoprecipitation—5×10^5 AtT-20 cells were used 40–48 h after seeding in 6-well plates. They were labeled with either 500 μCi/ml [^{35}S]methionine and -cysteine (Pro-Mix, Amersham Pharmacia Biotech) for 20 min or 500 μCi/ml [^{35}S]methionine (Amersham Pharmacia Biotech) for 8 h. Cells were then directly extracted or chased in DMEM containing 2% fetal bovine serum.

For the analysis of the maturation of mutant pro-PC2s, proteins were extracted under denaturing conditions, and immunoprecipitation was conducted at 4 °C as described previously (35). Briefly, extracts were first incubated for 1 h in the presence of protein A coupled to Sepharose CL-4B (Amersham Pharmacia Biotech). The pre-cleared supernatants were then incubated for 4 h in the presence of PC2 antiserum LSU18. The immune complexes were precipitated with protein A coupled to Sepharose CL-4B and washed once with the immunoprecipitation buffer, once with 0.5 M NaCl in phosphate-buffered saline, and twice with Dulbecco's modified Eagle's medium. They were then boiled in Laemmli sample buffer prior to separation by SDS-PAGE on 8.8% acrylamide gels. Gels were either treated for fluorography with Amplify (Amersham Pharmacia Biotech) or directly exposed to a phosphoscreen and analyzed using either a PhosphorImager (Storm, Molecular Dynamics, Sunnyvale, CA) and ImageQuant software (Molecular Dynamics) or on an InstantImager (Packard Instrument Co.).

For the *in vitro* analysis of pro-PC2 processing, cells were chased in DMEM containing 2% fetal bovine serum for 2, 4, or 12 h in the

presence of 1 μM bafilomycin A1 (Kamiya Biomedical Company, Seattle, WA). Proteins were then extracted under native conditions as described previously (41), and PC2 forms were immunoprecipitated as described above. The beads were then resuspended in 100 mM Bis-Tris, 100 mM sodium acetate at the indicated pH and incubated at 37 °C for 30 min. The reaction was stopped by adding Laemmli sample buffer and boiling for 5 min. Proteins were analyzed as described above.

In Vitro Activation of Pro-PC2 and HPLC Peptide Analysis—Pro-PC2 was purified from the medium of CHO cells expressing high levels of pro-PC2 and 7B2 as described previously (42). Pro-PC2 (~5–15 μg) was incubated in 100 mM Bis-Tris, 100 mM sodium acetate at the indicated pH at 37 °C. In some experiments the incubations were performed in the presence of 1 mM EDTA or 10 μM of the carboxyl-terminal peptide of 7B2 (CT peptide), a PC2-specific inhibitor (43). An aliquot was boiled in Laemmli sample buffer for Western blotting. Another aliquot was stopped by adding 4 volumes of 8 M urea and boiled for 5 min for the HPLC analysis of the fragments generated. Samples were fractionated on a C4 column (Vydac, Hesperia, CA) at a 1 ml/min flow rate using a three-step gradient consisting of 0–40% buffer B for 57 min, 40–70% B for 37 min, 70–100% B for 27 min, with buffer B being 80% acetonitrile with 0.06% trifluoroacetic acid and buffer A being 0.052% trifluoroacetic acid. 100-μl duplicate aliquots of each fraction were dried in the presence of carrier bovine serum albumin (BSA) and analyzed for PC2 propeptide content using a novel radioimmunoassay (RIA) using the LSU26 antiserum (see below). Amino-terminal peptide sequencing of the immunoreactive fractions was performed by the Protein and Carbohydrate Structure Facility (University of Michigan, Ann Arbor, MI), and matrix-assisted laser desorption ionization/time of flight-mass spectroscopy was performed by the LSU Core Labs (LSU Health Sciences Center, New Orleans, LA).

PC2 Assay—PC2 activity was measured using 0.2 mM pGlu-Arg-Thr-Lys-Arg-MCA (Peptides International, Lexington, KY) (final concentration) as a substrate as described previously (39). The assay was performed at 37 °C in 100 mM sodium acetate, pH 5, containing 5 mM $CaCl_2$ and 0.4% octyl glucoside, in the presence of a protease inhibitor mixture composed of 1 μM pepstatin, 0.28 mM tosylphenylalanine chloromethyl ketone, 1 μM *trans*-epoxysuccinic acid, and 0.14 mM tosyl-lysyl chloromethyl ketone (this inhibitor mixture was omitted when purified recombinant PC2 was used). In order to determine the enzymatic activity of the wild type and mutant PC2s, intracellular pro-PC2/PC2 was immunopurified from cell extracts (obtained by nondenaturing lysis from triplicate plates) using antiserum LSU18 bound to protein A-coupled Sepharose CL-4B. An aliquot of these same cell extracts was saved for protein determination using the BCA protein assay (Pierce), and similar amounts of cellular protein were subjected to Western blotting using antiserum against PC2 (LSU18). The activity of immunopurified enzymes prepared from the various cell lines was assessed under standard conditions for a 2-h reaction time and was normalized to the total intracellular content of PC2 forms expressed in that cell line. The entire experiment was repeated independently with similar results, and the results were also confirmed using overnight conditioned media from each cell line.

For analysis of inhibition by propeptide-related peptides, duplicate reactions were used, consisting of 7 nM mouse recombinant pro-PC2, 0 to 0.1 mM of the peptide to be tested, and 0.2 mM fluorogenic substrate. Prior to addition to the reaction mixture, purified recombinant mouse pro-PC2 was diluted in the assay buffer and preactivated by incubating for 30 min at 37 °C to obtain the 66-kDa form. Peptides corresponding to residues 57–84, 57–80 (containing an S57Y substitution), and 35–56 of mouse pro-PC2 were synthesized by LSU Health Sciences Center Core Labs. After preactivated PC2 was mixed with the peptide, the reaction mixtures were incubated at room temperature for 30 min, and the reaction was initiated by adding substrate followed by incubation at 37 °C for 30 min. The amount of released aminomethylcoumarin (AMC) was measured with a microtiter plate fluorometer (Ascent, Labsystems) using excitation and emission wavelengths of 380 and 460 nm, respectively. The amount of released product was calculated by reference to the fluorescence of free AMC standard. IC_{50} values were calculated by applying nonlinear regression to the data using the GraphPad Prism program. The values were determined from four independent experiments using two different PC2 preparations.

Active Site Titration of PC2—Purified pro-PC2 was activated at pH 5.0 for 30 min at room temperature prior to addition of 0.2 mM Glu(P)-Arg-Thr-Lys-Arg-MCA and varying (0–1 μM) quantities of decanoyl-Arg-Val-Lys-Arg-chloromethyl ketone (Alexis Biochemicals, San Diego, CA) under conditions such that $E_T \gg K_i^{app}$. Reactions were incubated at 37 °C. Least square regression was used to calculate E_T from the resulting quasi-linear plots as described by the Morrison equation (44).

Detection of Propeptide Molecular Forms in Mouse Brain, Cell Extracts, and Secretion Medium—Brains from wild type mice or from PC2 knockout mice (45) were directly homogenized on ice in 0.1 M HCl. Extracts were frozen, thawed, and centrifuged before lyophilization. Dried samples were then made up to 1.5 ml in 0.1% trifluoroacetic acid and centrifuged, and 500 μl of the clear supernatant was fractionated by HPLC. The propeptide was assayed in duplicate aliquots of each fraction by RIA, as described below.

AtT-20 cells, expressing PC2 alone or PC2 and 7B2, or Rin5f cells, expressing proenkephalin alone or with 7B2, were plated in 35-mm wells. Confluent cells were first incubated for 2 h under basal conditions. The medium was replaced for 3 more h, with fresh medium containing 100 nM phorbol 12-myristate 13-acetate (PMA). Collected media were spun to remove floating cells and directly assayed for propeptide immunoreactive by RIA. Cells were homogenized in 1 M acetic acid, 20 mM HCl, and 0.1% (v/v) β-mercaptoethanol. The extracts were frozen, thawed, centrifuged, and lyophilized before being subjected to the propeptide and α-MSH/ACTH-(1–13)-NH_2 or Met-enkephalin RIAs. In some experiments, the cell extracts or the stimulated medium were separated by HPLC as described above. Media were first concentrated using SepPak C18 columns (Waters, Milford, MA) eluted with 60% isopropyl alcohol, 0.1% trifluoroacetic acid and diluted in buffer A prior to application to the HPLC column. Aliquots of the HPLC fractions were dried together with 50 μl of 0.05% carrier BSA, and the propeptide content was measured by RIA.

Propeptide and Other Radioimmunoassays—Propeptide RIAs were carried out using 100 μl of a 1:40,000 dilution of antiserum LSU26, 100 μl of sample or standard, and 100 μl of iodinated peptide containing 10,000 cpm in RIA buffer consisting of 0.1 M sodium phosphate, pH 7.4, 0.1% heat-treated BSA, 0.1% sodium azide, and 50 mM sodium chloride. In order to enable iodination, the peptide to be radiolabeled (pro-PC2 58–80) was synthesized with the addition of an amino-terminal Tyr. This Tyr^{57}-substituted peptide was also used to generate the standard curve. The IC_{50} of the assay was 60 fmol, and the range of the standard curve was from 1 to 500 fmol. Other details of the RIA procedure were as described previously (46). Samples were subjected to carboxypeptidase B digestion prior to propeptide assay (42). The Met-enkephalin RIA has already been described (46).The α-MSH/ACTH-(1–13)-NH_2 RIA was accomplished using a 1:120,000 final dilution of antiserum (raised in sheep against α-MSH conjugated to thyroglobulin; Chemicon AB5087) and a standard curve of 1–250 fmol. Due to the specificity of the antibody for the amide moiety, cross-reaction was negligible for either intact ACTH, α-MSH-free acid, or ACTH-(1–10) (39).[2]

RESULTS

In Vitro Processing of Pro-PC2 Generates Intact Propeptide That Is Subsequently Internally Cleaved—Overall sequence conservation between the PC propeptides is quite low, as shown in Fig. 1, *panel A*. However, all propeptides are cleaved at a common R*X*KR locus, referred to as the primary site (Fig. 1, *panel B*), generating the mature PCs. In addition, all of the PCs except PC7 contain a second potential cleavage site, termed the internal site, located between 19 and 33 residues amino-terminal to the primary site. The internal site is not as well conserved as the primary site but contains a minimal recognition sequence of a basic doublet at positions 1 and 2, followed by additional basic residues at either positions 3 and/or 4, 5, and 6 (Fig. 1, *panel B*). A potential third site (the tertiary site) can also be seen in PC1, PC2, and furin and is located between the primary and internal sites, as shown in Fig. 1.

Recent data have demonstrated that profurin is first cleaved at the primary site, with hydrolysis of the internal site delayed until the enzyme reaches the acidic environment of the TGN (27). Whereas this mechanism may be applicable to many of the PCs, in the case of PC2 it has previously been shown that a form intermediate in size between the pro and mature forms can be generated (31, 33), implying that cleavage at the internal site may occur prior to cleavage at the primary site.

In order to investigate the processing of the PC2 propeptide,

[2] L. Muller, A. Cameron, Y. Fortenberry, E. V. Apletalina, and I. Lindberg, unpublished results.

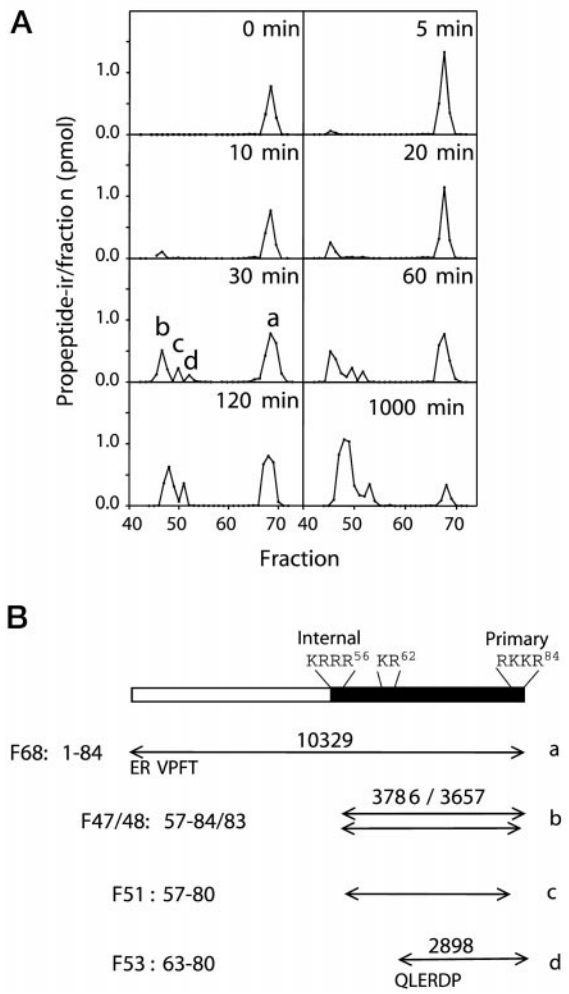

FIG. 2. **The pro-PC2 propeptide is internally cleaved during *in vitro* activation of pro-PC2.** *Panel A,* detection of immunoreactive propeptide in HPLC fractions from *in vitro* activated pro-PC2. Pro-PC2 was activated at pH 5 at 30 °C for different times. The reaction products were separated by HPLC as described under "Materials and Methods." Propeptide immunoreactive fragments were measured by RIA. The peaks (*a–d*) are indicated for the 30-min sample. *Panel B,* identification of the HPLC peaks. The HPLC immunoreactive peaks were identified either by (i) mass spectroscopy (*peaks a, b,* and *d*); mass is indicated above the *double-arrow* denoting the peptide; (ii) amino-terminal amino acid sequencing (*peaks a* and *d*); the experimental sequence is shown under the peptide; or (iii) HPLC spiking/RIA of the synthetic peptides (*peak c*). The fraction number and the elution position of the peptides are indicated on the *left.*

we used recombinant mouse pro-PC2 purified from the medium of CHO cells co-expressing 7B2 (38). *In vitro*, this pro-PC2 rapidly converts into active mature PC2 in an autocatalytic process that is strictly pH-dependent (47). To study this process better, we reduced the rate of conversion by incubating reactions at 30 °C, rather than 37 °C, for varying times. The reaction products were then separated by HPLC, and the fractions were analyzed by RIA using an antiserum (LSU26) directed against the region of the propeptide between the two cleavage sites (residues Leu^{58}–Asp^{80}, represented by a *hatched box* in Fig. 1, *panel B*). Cross-reaction studies using the basic residue-extended peptide Ser^{57}–Arg^{84} showed a 2–3-fold increase in immunoreactivity in the propeptide RIA following treatment with carboxypeptidase B. Consequently, all HPLC fractions were routinely carboxypeptidase B-treated to maximize sensitivity and to eliminate any differences arising from the presence of carboxyl-terminal basic residues.

As shown in Fig. 2, *panel A*, the initial major immunoreactive peak, *peak a*, was seen to increase in size for the first 5 min and then to slowly decrease; by the last time point it accounted only for a small percentage of the total immunoreactivity. In contrast, *peak b* increased steadily until it became the major immunoreactive peak. After incubation times of 30 min or longer, two minor peaks, labeled *c* and *d*, could also be detected.

Fig. 2, *panel B,* describes the locations/assigned identities of the fractions containing immunoreactive peptides within the PC2 propeptide. Peak a was identified as the intact propeptide by both amino-terminal sequencing and matrix-assisted laser desorption ionization/time of flight mass spectroscopy. Peak b was identified by mass spectroscopy as the peptide corresponding to residues Ser^{57}–Arg^{84}, one of the fragments predicted by cleavage at the internal site; however, weak signals from the mass spectrometer implied that Ser^{57}–Lys^{83} was also present in this fraction. Peak c co-migrated with a synthetic peptide Ser^{57}–Asp^{80}, whereas peak d was identified as Gln^{63}–Asp^{80} by sequencing and mass spectroscopy. Peak d was also observed when these experiments were repeated in the presence of guanidino(ethylmercapto)succinic acid or *o*-phenanthroline, both inhibitors of carboxypeptidases.[2] Additional data generated from limited carboxypeptidase B digestions of synthetic Ser^{57}–Arg^{84} peptide showed separation of peptide products into four well separated peaks using this HPLC method, which corresponded to (i) a mixture of Ser^{57}–Arg^{84} and Ser^{57}–Lys^{83}; (ii) Ser^{57}–Lys^{82}; (iii) Ser^{57}–Arg^{81}; and (iv) Ser^{57}-Asp^{80}, as demonstrated by mass spectroscopy (data not shown).

The results presented above demonstrate the sequence of propeptide cleavage as follows: first at the primary site, then at the internal site, and finally at the tertiary site. In addition to endoproteolytic cleavage, we also observed exoproteolytic processing of carboxyl-terminal basic residues generating the Ser^{57}–Asp^{80} peptide and the Ser^{57}–Arg^{83} peptide. Interestingly, we did not detect any intact propeptide that had been carboxyl-terminally trimmed (*i.e.* a peak corresponding to Glu^{1}–Asp^{80}), yet the product of cleavage at the tertiary site was only observed in the trimmed state, implying that cleavage at the tertiary site occurs after exoproteolytic trimming of the primary site basic residues.

In Vitro, Internal Cleavage of the Propeptide Is Intramolecular and Rapid—To analyze the mechanism of internal processing of the PC2 propeptide, we incubated pro-PC2 at pH 5 in the presence of EDTA or of the 7B2 CT peptide, a specific and potent inhibitor of PC2. Previous results demonstrate that neither compound is able to block the autocatalytic activation (47), suggesting an intramolecular mechanism for propeptide removal. In our hands, these agents were also unable to inhibit the propeptide internal cleavage event (results not shown). In order to determine whether internal propeptide cleavage was inter- or intramolecular, we incubated iodinated intact propeptide, prepared from *in vitro* incubation of purified pro-PC2 and separated by HPLC, in the presence of activated PC2 at pH 5 and 37 °C. Processing of the iodinated propeptide was negligible, even after overnight incubation (results not shown). These data strongly suggest that internal processing of the propeptide is strictly intramolecular. To determine whether internal cleavage of the propeptide is necessary for the acquisition of enzymatic activity, we compared the kinetics of acquisition of enzyme activity against a fluorogenic substrate to those of cleavage of the internal site (Fig. 3). PC2 activity was maximal after 30 min, by which time the internally cleaved propeptide forms accounted only for some 40% of the total immunoreactive propeptide fractions. Indeed, even after overnight incubation only 80% of the propeptide was internally processed. However, active site titration of the purified pro-PC2 preparation with decanoyl-Arg-Val-Lys-Arg-chloromethyl ketone (data not

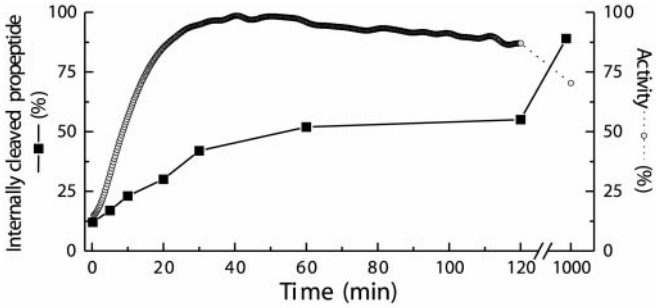

FIG. 3. **Internal cleavage of the propeptide *in vitro* is correlated with pro-PC2 activation at early, but not at later, time points.** Pro-PC2 was incubated at pH 5 for different times at 30 °C. At the end of the incubation, propeptide fragments generated were separated by HPLC and assayed by RIA. The amount of internally cleaved propeptide is expressed as a percentage of the total immunoreactive propeptide fragments. The hydrolysis of Glu(P)-Arg-Thr-Lys-Arg-MCA by PC2 at pH 5 and 30 °C was measured every 15 s, and the resulting units of fluorescence were integrated to obtain the rates at individual time points. The latter data represent the Savitzky-Golay smoothed (n = 10) mean of three independent experiments. The total hydrolysis of the substrate was less than 7% after 2 h. The rate at the 1000-min time point was obtained by assaying an aliquot incubated separately. Results are expressed as the percentage of the maximum activity measured by the release of AMC, as described under "Materials and Methods."

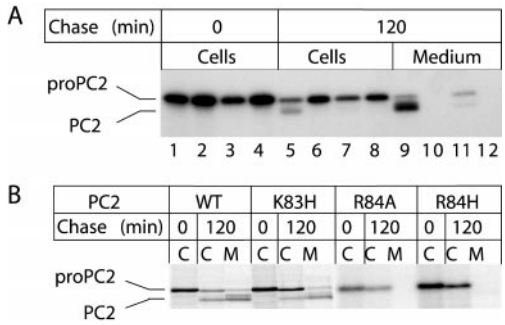

FIG. 4. **Internal cleavage of the propeptide is not required for generation and secretion of mature PC2 *in vivo*.** *Panel A,* processing of pro-PC2 propeptide cleavage site mutants. Wild type pro-PC2 (*lanes 1, 5,* and *9*) and pro-PC2 mutated within the four residues of the primary cleavage site (M81-84) (*lanes 2, 6,* and *10*), pro-PC2 mutated within the internal site (M53-56) (*lanes 3, 7,* and *11*), or the double mutant pro-PC2 (2M) (*lanes 4, 8,* and *12*) were co-expressed with 7B2 in AtT-20 cells. Cells were metabolically labeled for 20 min and either directly extracted or chased for 120 min. Pro-PC2 and PC2 were immunoprecipitated, and proteins were separated by SDS-PAGE and subjected to autoradiography. *Panel B,* processing of pro-PC2 primary cleavage site point mutants. Wild type pro-PC2 and pro-PC2 mutated at the P2 Lys (K83H) or at the P1 Arg (R84H and R84A) were co-expressed with 7B2 in AtT-20 cells. Pro-PC2 processing and secretion were determined as in *panel A.* The gels were analyzed using a PhosphorImager.

shown) or the tight binding specific inhibitor 7B2 CT (38) indicates that a substantial proportion of purified recombinant PC2 is catalytically inactive. The agreement between the shapes of the two curves at early time points leads us to suspect that the initial rapid internal cleavage of propeptide is derived from the active pro-PC2 fraction (40%), whereas the subsequent slow cleavage may represent internal cleavage of propeptide from an inactive pro-PC2 form (60%). If only the initial time points are considered, the data support the idea that the internal propeptide cleavage occurs with a time frame compatible with the acquisition of enzyme activity, *i.e.* activation. Alternatively, because of the need to use relatively high concentrations of pro-PC2 in these experiments, internal propeptide cleavage could occur so rapidly after activation as to be kinetically indistinguishable from the latter process.

Mutation of the Internal Cleavage Site Does Not Prevent Pro-PC2 Activation—To allow us to analyze the relationship between internal propeptide cleavage and the mechanism of pro-PC2 activation *in vivo*, we used directed mutagenesis. We initially mutated the four residues of the pro-PC2 internal site (residues 53–56, KRRR to KHKH) and primary site (residues 81–84, RKKR to KHKH). Mutated pro-PC2s were expressed in AtT-20 cells stably expressing 7B2 in order to provide an optimum level of pro-PC2 maturation (35). The mutants were analyzed for the maturation of pro-PC2 into PC2 and for the secretion of PC2 into the medium. Fig. 4, *panel A,* shows that whereas the cells expressing wild type pro-PC2 released mainly mature PC2, pro-PC2 was the major form secreted by cells expressing the M53-56 mutant. Thus mutation of the internal site affected the folding rate of pro-PC2, as shown by the low level of mature M53-M56 PC2 in both the cells and the secretion medium (Fig. 4, *panel A*). In addition, the intermediate 71-kDa PC2 could not be detected in cells expressing pro-PC2 with the internal site mutation,[3] confirming that the internal cleavage of the propeptide actually does occur at KRRR^{56}.

Mutation of the four residues of the primary site (M81-84) resulted in the synthesis of an unstable form of proenzyme that was degraded intracellularly (Fig. 4, *panel A*). Even in a clone that expressed a higher level of mutant pro-PC2 than wild type pro-PC2 in the control cells, we could not detect any mature PC2. As expected from this result, the mutation of both the primary and the internal sites (2M) had the same effect, *i.e.* accumulation and slow degradation of pro-PC2 within the cells. These results suggest that the mutation of the primary site prevents the proper folding of pro-PC2 in the ER, in agreement with previous studies using directed mutagenesis of the propeptide of furin, PC1, and PC2 (12, 48, 49) and with the proposed role of the PC propeptide as an intramolecular chaperone (for review of propeptides as intramolecular chaperones see Ref. 25).

Unlike Primary Site P2 Mutants, Internal Site Mutants Are Autocatalytically Processed—As mutation of all four primary site recognition sequence residues prevented processing and secretion, we mutated only the P1 and P2 residues into His or Ala (R84H, R84A, and K83H). Although K83H PC2 (a P2 position mutant) was processed and secreted, P1 position mutants were not (Fig. 4, *panel B*). We conclude that the P1 position in the primary site is critical to propeptide processing.

The distinction between autocatalytic removal of propeptide and actual activation of the subtilases is an important one. For example, certain catalytic domain mutants of subtilisin (50), furin (51), and PC2 (36) retain the capacity to process autocatalytically their propeptides but cannot cleave other substrates. Another example is the pattern of expression of pro-PC2 in CHO cells lacking 7B2, in which a certain amount of mature PC2 is secreted in the absence of any detectable catalytic activity (33).

In order to study the proteolytic maturation of the pro-PC2s described above that were mutated in the propeptide domain, we designed an *in vitro* assay to determine if processing occurred through an intra- or intermolecular mechanism. In this assay, radiolabeled native and mutant pro-PC2s are immunopurified under native conditions from extracts of AtT-20/7B2 cells that are unable to undergo PC2 propeptide processing *in vivo* (*i.e.* bafilomycin treatment). Following immunopurification, the proenzymes are incubated *in vitro* either at pH 5 to permit propeptide processing to proceed or at pH 7 to prevent processing. The reaction products are then analyzed by SDS-PAGE and autoradiography to assess the degree of propeptide processing that has occurred.

[3] L. Muller, unpublished results.

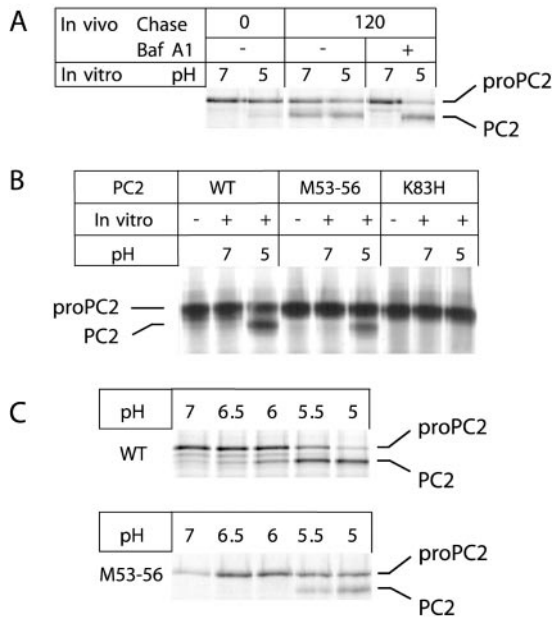

FIG. 5. **Pro-PC2 mutated in the primary cleavage site is not autocatalytically processed.** *Panel A, in vitro* autocatalytic processing of immunopurified pro-PC2. AtT-20 cells that stably co-express pro-PC2 and 7B2 were metabolically labeled for 20 min and either directly extracted or chased for 120 min under control conditions or in the presence of 1 μM bafilomycin A_1. Pro-PC2 and PC2 were immunopurified and incubated at pH 7 or 5 for 30 min at 37 °C. Proteins were separated by SDS-PAGE, and gels were analyzed with a PhosphorImager. *Panel B,* M53-56 is autocatalytically processed *in vitro*, whereas K83H is not. AtT-20 cells that stably co-express 7B2 and either wild type or M53-56 or K83H mutant pro-PC2 were metabolically labeled for 20 min and chased for 120 min in the presence of 1 μM bafilomycin A_1. Radiolabeled pro-PC2 was immunopurified and submitted to electrophoresis either directly or after a 30-min *in vitro* incubation at pH 7 or 5. Proteins were separated by SDS-PAGE and subjected to autoradiography. *Panel C,* pH dependence of M53-56 *in vitro* processing. AtT-20 cells that stably co-express 7B2 and either wild type (*WT*) or M53-56 mutant pro-PC2 were metabolically labeled for 20 min and chased for 120 min in the presence of 1 μM bafilomycin A_1. Pro-PC2 maturation was analyzed at the indicated pH.

At the end of a 20-min labeling period, immunopurified wild type pro-PC2 showed no change after *in vitro* incubation at pH 5 for 30 min at 37 °C, the great majority of protein remaining in the higher molecular weight zymogen form. However, following a 120-min chase period, both the zymogen and mature forms were present, with only a slight increase in the mature form after *in vitro* incubation at pH 5 (Fig. 5, *panel A*). Note that incubation at pH 7 did not result in processing of pro-PC2 (compare the *2nd lane* in Fig. 4, *panel B,* with the *3rd lane* in Fig. 5, *panel A*; see also Fig. 5, *panel B*). These results were expected, because a requirement for pro-PC2 activation is correct folding in the ER, a process that has been shown to be relatively slow (41). In addition, the lack of substantial processing of radiolabeled pro-PC2 by the co-immunopurified cold PC2 confirms the intramolecular mechanism of pro-PC2 processing previously proposed (Refs. 38 and 52 and this work). These results also support our previous finding that, once folded, pro-PC2 is rapidly transported to the TGN/secretory granules where it is activated (41).

In light of these results, we incubated cells under conditions that block *in vivo* processing (41) by treating the cells with bafilomycin A_1, an inhibitor of the vacuolar H^+-ATPase present in the membranes of the TGN and the secretory granules. The *last 2 lanes* of Fig. 5, *panel A,* show that, after a 120-min chase in the presence of bafilomycin A_1, processing had not occurred *in vivo* but could be instigated *in vitro* by lowering the pH to 5. Similarly to the autocatalytic processing of pro-PC2 (38), this *in vitro* processing did not require the presence of calcium and was not prevented by the presence of 1 μM CT peptide (data not shown).

TABLE I

Enzymatic activity of immunopurified wild type and mutant PC2s

Pro-PC2/PC2 forms were immunopurified from cell extracts and subjected to the standard PC2 assay. Results (mean + S.D. of triplicate determinations) were normalized for PC2 expression in that cell line.

Cell line	PC2 activity
	pmol AMC/h
AtT-20/PC2	18.5 ± 4.8
AtT-20/PC2/7B2	160 ± 20
AtT-20/PC2 M53–56/7B2	120 ± 5.4
AtT-20/PC2 K83H/7B2	1.2 ± 0.7

Whereas the M53-56 internal mutant was not as extensively processed as wild type pro-PC2, processing was still autocatalytic and pH-dependent (Fig. 5, *panels B* and *C*). The *in vivo* processing and the secretion of the M53-56 pro-PC2 seemed to occur more slowly than for wild type pro-PC2 (Fig. 4, *panel A*). Thus, we investigated the *in vitro* processing of this mutant after longer chase times of the cells in the presence of bafilomycin A_1 (in order to allow additional time for folding of this mutant). However, extending the chase for up to 12 h did not result in the production of more than 30% of mature M53-56 mutant PC2 *in vitro*. These data suggest that the folding of M53-56 mutant pro-PC2 was less efficient rather than simply slower.

Mutation of the primary site P2 lysine (K83H) also resulted in a proenzyme that could be transported out of the ER and processed *in vivo* (Fig. 4, *panel B*). However, when cells expressing the K83H mutant were chased in the presence of bafilomycin A_1, *in vivo* processing of its propeptide was not observed. These results demonstrate that the cleavage of the propeptide of the K83H mutant is pH-dependent *in vivo,* similar to that of the wild type pro-PC2 (compare Fig. 4, *panel B*, *lane 5*, and Fig. 5, *panel B, lane 7*). Unlike the internal site mutant, the single-point primary site K83H mutant did not undergo *in vitro* autocatalytic processing (Fig. 5, *panel B*). Extending the chase time in the presence of bafilomycin A_1 up to 12 h also did not result in any *in vitro* autoprocessing of this mutant. These data suggest that the *in vivo* processing of this mutant was not autocatalytic, instead potentially resulting from the activity of another enzyme such as furin or PC1.

We also investigated the enzymatic activity of the mutant PC2s immunopurified from AtT-20 cells co-expressing 7B2. Control cells expressing either wild type PC2 or wild type PC2 and 7B2 were also examined. Whereas the internal site M53-56 mutant was about 70% as active as the wild type enzyme, we could not detect enzymatic activity (as assessed by cleavage of a fluorogenic substrate) for the primary site K83H mutant (Table I). These data are in agreement with our proposed activation mechanism of the mutant PC2s; M53-56 PC2 is autocatalytically processed and is active, whereas K83H is not autocatalytically processed and is not active.

Taken together, the results described above demonstrate that *in vivo*, internal cleavage of the PC2 propeptide is not an obligatory intermediate step in the pro-PC2 maturation pathway and is not required for PC2 activation. In addition, our directed mutagenesis experiments demonstrate the involvement of the propeptide cleavage sites in various levels of pro-PC2 folding. Even though the internal site (M53-56) and single-point primary site (K83H) mutants were both sufficiently well folded to pass through ER quality control, the internal site mutation apparently lowered the efficiency of the folding of the catalytic domain but did not prevent the autocatalytic processing and activation of this mutant pro-PC2. On the other hand,

TABLE II
Inhibition constants for PC2 propeptide-related peptides against PC2

The rate of hydrolysis of pERTKR-AMC by purified mPC2 was determined in the presence of varying concentrations (0–100 μM) of the synthetic peptides. The results obtained were used to calculate the IC_{50} values using nonlinear regression. Values shown are the mean ± the S.D. obtained from 2 to 3 independent experiments.

Peptide	IC_{50}
	μM
Peptide N1 (residues 35–56)	>100
Peptide N2 (residues 58–84)	2.4 ± 0.3
Peptide N3 (residues 57–80)	>100

the K83H mutation generated a PC2 molecule with a completely inactive catalytic domain, even though the mature enzyme itself contained no mutation.

A PC2 Propeptide Fragment Terminating in Basic Residues Is a Potent Inhibitor of PC2 Activity—The propeptides of furin and PC1 have been shown to be potent inhibitors of their cognate enzymes (27, 28). In agreement with these studies, preliminary data show that HPLC fractions, originating from incubation of recombinant pro-PC2 and shown by mass spectroscopy to contain the intact PC2 propeptide, were inhibitory to PC2.[2] In order to identify the inhibitory site in the propeptide and to quantify the extent of inhibition, we tested three synthetic peptides against recombinant PC2. The N1 peptide (residues Leu^{35}–Arg^{56}) contained the KRRR internal cleavage site; N2 (residues Ser^{57}–Arg^{84}) contained the RKKR primary site as well as the KR^{62} site; and N3 (Tyr–Leu^{58}–Asp^{80}) was trimmed of the four carboxyl-terminal basic residues (and thus containing only the KR^{62} tertiary cleavage site). The data in Table II show that only the N2 peptide was inhibitory to PC2. As N2 corresponds to the carboxyl-terminal portion of the propeptide, complete with basic residues, these results indicate that the primary cleavage site is required for inhibitory potency. These data are in agreement with a recent report identifying the carboxyl-terminal peptides of the furin and PC7 propeptides as the inhibitory sites (29). Interestingly, the carboxyl-terminal hexapeptide of N2 exhibited 6-fold reduced inhibitory potency,[4] indicating that PC2 possesses an extensive binding site for the propeptide.

Propeptide Immunoreactivity in Brain and in AtT-20 Cells Transfected with Pro-PC2 Consists of Internally Cleaved Propeptide—The data above identify the inhibitory forms of the propeptide active *in vitro*; we next investigated which forms of the propeptide are present *in vivo*. For this purpose, we determined the molecular forms present in mouse brain and in transfected AtT-20 cells. Brains were extracted into 0.1 M HCl and separated by HPLC prior to propeptide RIA (Fig. 6, *panel A*). In order to characterize the peaks, independent samples were spiked with picomole quantities of either the Ser^{57}–Arg^{84} or the Ser^{57}–Asp^{80} peptides. The peak present in fraction 52 co-migrated with the Ser^{57}–Asp^{80} peptide, *i.e.* the carboxyl-terminal internally cleaved propeptide trimmed of the carboxyl-terminal basic residues from the primary cleavage site. This propeptide fragment thus was expected to have no inhibitory potency. In addition, another immunoreactive peak was detected in fraction 56. In order to confirm that this peak specifically corresponded to a PC2 propeptide fragment, we performed the same experiment using brain extracts from PC2 null mice (45). As expected, no immunoreactivity was detected in any fraction from these brain extracts. Although we cannot definitively identify the immunoreactive peak detected in fraction 56, it may possibly correspond to the peptide Gln^{63}–Asp^{80} (generated by cleavage at the tertiary site) detected in the *in vitro* experiments (see Fig. 2, *panel A, peak d*).

[4] E. V. Apletalina, unpublished results.

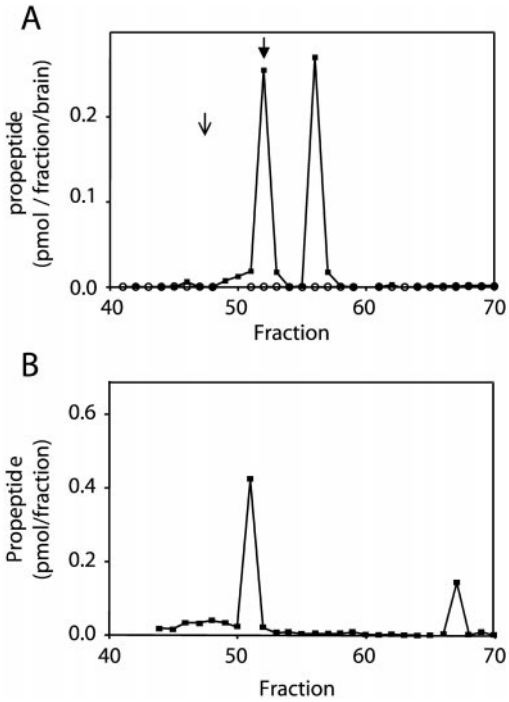

FIG. 6. **In mouse brain and in AtT-20 cells the propeptide is mainly present as an internally cleaved peptide with no carboxyl-terminal basic residues.** *Panel A,* brain tissue. Brain tissue from wild type (*closed squares*) or PC2 null mice (*open circles*) was acid-extracted, and extracts were subjected to reverse phase HPLC. Immunoreactive propeptide fragments were measured by RIA. The positions at which the 57–80 and the 57–84 peptides elute are indicated by a *closed* and an *open arrow*, respectively. *Panel B,* AtT-20 cells. AtT-20 cells overexpressing pro-PC2 and 7B2 were acid-extracted, and the propeptide forms were analyzed as in *panel A.*

We also investigated the immunoreactive propeptide forms present in AtT-20 cells expressing PC2 and 7B2. The major immunoreactive peak also corresponded to the carboxyl-terminally trimmed Ser^{57}–Asp^{80} peptide (Fig. 6, *panel B*). In addition, these cells contained minor amounts of the intact propeptide. The same pattern was observed with AtT-20 cells expressing PC2 in the absence of added 7B2 (data not shown). Therefore, these data strongly suggest that the main propeptide forms present *in vivo* are the two internally cleaved propeptide forms trimmed of basic residues and thus are inactive with respect to the ability to inhibit PC2.

The Intracellular Fate of the PC2 Propeptide—Although information concerning the inhibitory potency of the propeptide of the PCs has been reported, and association of the furin propeptide with mature furin has been observed (27–29), the intracellular fate of the propeptide after loss of inhibitory potency has not yet been described. The propeptide fragment is mainly generated in the TGN/immature secretory granules (for review see Ref. 30).

In order to study the sorting of the propeptide, we measured secretion under basal and stimulated conditions in AtT-20 cells overexpressing either PC2 alone or PC2 and 7B2. Secretion was measured under basal conditions and after a 2-h period in the presence of the secretagogue PMA. In both AtT-20/PC2 and AtT-20/PC2/7B2 cell lines, the secretion of immunoreactive propeptide was stimulated (Fig. 7, *panel A*). In order to evaluate the stimulatory effect of PMA on the propeptide release, the secretion of ACTH-(1–13)-NH_2 was measured using an α-MSH RIA which also detects unacetylated MSH (*i.e.* ACTH-(1–13)-NH_2). ACTH-(1–13)NH_2 is known to represent a pro-opiomelanocortin-derived PC2 processing product in PC2-transfected

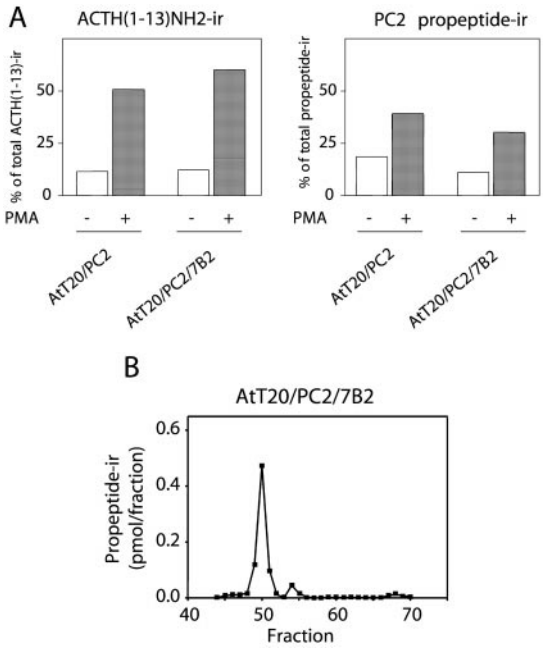

FIG. 7. **The propeptide is secreted through the regulated secretory pathway as an internally cleaved form.** *Panel A,* stimulated secretion of propeptide and ACTH-(1–13)-NH_2 immunoreactive (*ir*). AtT-20 cells expressing pro-PC2 alone or pro-PC2 and 7B2 were plated in 6-well plates. Cells were first incubated in serum-free medium for 2 h. Medium was replaced and collected after a 3-h chase under basal conditions (chase 1). Medium was replaced by fresh medium containing 100 nM PMA for 3 more h (chase 2). The medium of both basal release and stimulated release was then assayed for the presence of the PC2 propeptide and ACTH-(1–13)-NH_2, which was used here as a control for secretion. Results are expressed as the percentage of the total peptide (*i.e.* chase 1 + chase 2 + cells). *Panel B,* identification of released propeptide forms. AtT-20 cells co-expressing pro-PC2 and 7B2 were seeded in a 10-cm dish and incubated in the presence of 1 μM PMA for 3 h. The medium was concentrated using a SepPak column (Waters) and separated by HPLC. Fractions were assayed for propeptide immunoreactivity by RIA.

AtT-20 cells (53). Therefore, ACTH-(1–13)-NH_2 is generated in the secretory granules after the propeptide has been removed, and PC2 has been activated. These experiments demonstrated that the stimulation of the secretion of the propeptide is not as efficient as that of the peptides present in the secretory granules, ~4-fold for ACTH-(1–13)NH_2 and ~2-fold for the PC2 propeptide (see Fig. 7, *panel A*). In addition, we investigated the molecular forms of propeptide released by AtT-20 cells expressing PC2 and 7B2. The Ser^{57}–Asp^{80} internally cleaved peptide lacking carboxyl-terminal basic residues was the major propeptide form released (Fig. 7, *panel B*). This result is in agreement with the molecular forms identified in these cells (see Fig. 6). An identical result was observed in AtT-20 cells expressing PC2 in the absence of stably transfected 7B2.

Taken together, these experiments demonstrate the presence of internally cleaved and carboxyl-terminally trimmed PC2 propeptide in secretory granules.

DISCUSSION

The propeptides of zymogens from the various protease families act as regulators of both the activation and the activity of their cognate enzymes. These domains are thus key components of the proteolytic machinery used by cells to regulate the processing of precursors. In the present work, we were able to demonstrate the involvement of PC2 propeptide at different steps of pro-PC2 activation. The propeptide is directly involved in the folding of the PC2 catalytic site and can act as an inhibitor of active PC2; inhibitory potency is terminated by the exoproteolytic processing of the basic residues in the primary cleavage site. In addition, our *in vivo* analysis of the processing of pro-PC2 and of the propeptide demonstrates that the internal cleavage of the propeptide is not strictly required for PC2 activation, unlike the process described for furin (27). Finally, the internally cleaved propeptide is stored in secretory granules and undergoes stimulated secretion.

The PC2 Propeptide Acts as an Intramolecular Chaperone—The PC propeptide fulfills the characteristics of an intramolecular chaperone; it is required for the activation of the zymogen but is itself not part of the active form (for review see Refs. 23–25). A role for PC propeptides as active intramolecular chaperones has, however, not yet been demonstrated. The intramolecular chaperone function of zymogen propeptides has been demonstrated *in vitro* in denaturing/renaturing experiments and *in vivo* by co-expressing the propeptide and the mature enzymes in *trans* (for review see Refs. 23–25). One of the limits of studying PCs is the lack of purified zymogen that can be activated *in vitro*, as only pro-PC2 can be purified as a zymogen (38). We used purified pro-PC2 in extensive denaturing/renaturing experiments but were unable to recover any enzymatic activity even after only partial denaturation.[5,6] These experiments, performed both in the presence or absence of the PC2-specific binding protein 7B2, suggested that pro-PC2 folding is a complex reaction that may require other factors, such as ER molecular chaperones. The inability to refold *in vitro* is not unexpected given the large size of the convertase zymogens (70–100 kDa) compared with prosubtilisin (35 kDa).

Directed mutagenesis is thus the only approach that can generate information concerning the function of the PC propeptides as intramolecular chaperones, and previous studies involving directed mutagenesis have supported the idea that the PC propeptides indeed function as intramolecular chaperones (12, 49). However, propeptide mutant proenzymes are retained in the ER (12, 49); therefore, these experiments show that the PC propeptide is generally required for proper folding of the zymogen but not that it is specifically involved in the generation of a properly folded catalytic pocket.

The specificity of PC2 for its own propeptide was first demonstrated by exchanging the propeptides of furin, PC1, and PC2 (48). Large deletions of 8–50 residues inside the propeptide sequence resulted in the retention of the mutated pro-PC2 in the ER (49). Deletion or point mutations inside the primary cleavage site of furin or PC2 demonstrated that the integrity of this cleavage site is required for the exit of these proteins from the ER (12, 49), suggesting that this portion of the propeptide is required for the proper folding of the zymogen. In our experiments, mutation of the four residues in the primary cleavage site, or solely of the P1 Arg within this site, resulted in intracellular degradation. On the other hand, mutation of only the P2 Lys within the primary cleavage site did not prevent the proper transport of pro-PC2 out of the ER into the Golgi nor the pH-dependent removal of the propeptide, although our *in vitro* processing data show that the latter event cannot be accomplished autocatalytically. Mature PC2 which is generated from the P2 Lys mutant was, however, catalytically inactive. These results provide evidence for the role of the propeptide, and specifically of the primary cleavage site, as an intramolecular chaperone directly involved in the local folding of the PC2 catalytic site. A similar role for the carboxyl-terminal basic residues of the Kex2p propeptide has also recently been proposed (27). No structural data are available for any PC thus far, but crystal structures have been obtained for either the propeptide/mature enzyme complex or the zymogen of a wide range of

[5] A. Cameron and I. Lindberg, unpublished data.
[6] J. Bruno and I. Lindberg, unpublished data.

enzymes such as carboxypeptidase B (54), procathepsin B (55), pepsinogen (56), and, more relevantly to the PCs, subtilisin (57). A common feature of these structures is the presence of the propeptide cleavage site buried within the catalytic cleft. Our results are in agreement with such a conformation for pro-PC2 and suggest that the primary cleavage site may be involved in the folding of PC2 by acting as a template for the catalytic site, recently described for subtilisin as "protein memory" (58, 69).

Pro-PC2 Processing and Activation—Whereas the processing of all other PCs generates only one molecular species, *i.e.* the mature form of the enzyme cleaved at the R*X*KR primary site (Fig. 1), two molecular forms result from the processing of pro-PC2, including the major 71-kDa intermediate (31, 33). Our analyses of the pro-PC2 processing mechanism *in vitro*, using purified pro-PC2, and *in vivo*, using directed mutagenesis of the cleavage sites, demonstrate that the activation of pro-PC2 occurs through the ordered processing of the zymogen at the $RKKR^{87}$ primary site, followed by the internal cleavage of the propeptide at $KRRR^{56}$ and KR^{63}. These results suggest that the 71-kDa form of mature PC2 is not relevant to the activation mechanism and could result from an alternate processing pathway that involves another protease, such as furin. In agreement with this possibility, the generation of the 71-kDa PC2 form did not require acidification of the pH, as it was produced in cells treated with bafilomycin A_1 (Fig. 5, *panel A, lane 5*).

Directed mutagenesis of the internal cleavage site of the PC2 propeptide did not prevent activation of pro-PC2; this situation is dissimilar to the results obtained with mutagenesis of profurin, which demonstrated the requirement for the internal cleavage of the propeptide for furin activation (27). Activation through an intramolecular autocatalytic processing event was proposed for the PCs using directed mutagenesis (51, 52, 59) and *in vitro* activation of purified pro-PC2 (38, 47). The present work further dissects the activation mechanism by showing that internal cleavage of the propeptide also occurs through an autocatalytic processing event, as EDTA or the CT peptide inhibitor could not block this processing step nor could iodinated propeptide be internally cleaved by activated PC2. The exact molecular mechanism of the internal propeptide cleavage event requires further study. By comparison, the extensive body of work that has been generated using prosubtilisin and procathepsins has indicated the presence of both intra- and intermolecular pathways of internal propeptide cleavage (19, 60–62).

Internal processing of the propeptide through an intramolecular pathway requires that certain conformational rearrangements take place after cleavage of the primary site, in order to insert the internal cleavage site in the catalytic pocket. Such a conformational change could be generated by propeptide pH sensitivity in the vicinity of the internal cleavage site. Indeed, whereas the amino-terminal portion of the propeptide (residues Glu^1–Ala^{52}) has a slightly acidic calculated pI (6.15), the carboxyl-terminal segment (residues Ser^{57}–Asp^{80}) has a very basic pI (9.95). Zymogen propeptides are known to be randomly structured and to acquire secondary structure only through binding to their cognate enzymes, as in the case of subtilisin (63), matrix metalloproteases (64), or cathepsin L (65). Thus, the exposure of pro-PC2 to acidic pH could first trigger cleavage at the primary site, followed by a pH-induced conformational change within the propeptide which then inserts the internal site into the catalytic pocket and results in autocatalytic internal site cleavage. This scenario stands in contrast to the previously proposed hypothesis of acid-induced histidine protonation causing dissociation of internally cleaved propeptide as the molecular mechanism responsible for the activation of furin (24). While displacement of the primary site by the internal site of the PC2 propeptide may indeed be required, in contrast to furin, actual internal cleavage of the PC2 propeptide is apparently not critical to activation, since internal cleavage site mutants can generate active enzyme.

The Propeptide Inhibits PC2 Activity—Propeptide-mediated inhibition is a common feature of many enzymes (for review see Ref. 22). We have shown here that a 27-residue PC2 propeptide fragment added in *trans* is an inhibitor of PC2 activity, as previously demonstrated for furin and PC1 and PC7 (27–29, 66). Interestingly, the PC2 propeptide fragment was not nearly as potent as these other PC propeptides and fragments of the same size (micromolar *versus* nanomolar inhibitory potency). This result should be moderated, however, by the fact that PC2 is also specifically inhibited in the nanomolar range by another endogenous peptide inhibitor, the 7B2 CT peptide (43, 67). Our data identify the inhibitory site of the propeptide as the basic residues that are carboxyl-terminally exposed after cleavage of the primary site, in agreement with a recent study concerning the furin and PC7 propeptides (29). Our data also suggest that the inhibitory potency of the propeptide is terminated by the action of a carboxypeptidase, most likely carboxypeptidase E, which is known to be present within secretory granules (68). In agreement with this idea, we identified the main propeptide molecular forms present in the brain as the internally processed and carboxyl-terminally trimmed peptides. We speculate that the rapid replacement of the primary cleavage site by the internal cleavage site in the catalytic pocket that occurs upon pro-PC2 activation would also result in exposure of the primary site carboxyl-terminal basic residues to carboxypeptidase E, thus terminating propeptide inhibition.

The Intracellular Fate of the Propeptide—Many studies have previously proposed that PC2 propeptide removal is initiated in the TGN and occurs mainly in the immature secretory granules (for review see Ref. 30). The major intracellular and secreted molecular form we detected was the internally processed and carboxyl-terminally trimmed propeptide. The presence of this propeptide species in the secretory granules was demonstrated by its ability to undergo stimulated secretion. However, the 2-fold elevation of propeptide immunoreactivity seen upon stimulation was lower than the 4-fold stimulation observed for prohormone processing products. This latter result implied that a portion of the PC2 propeptide may be partially sorted out of the maturing secretory granules. We thus further investigated the intracellular localization of the propeptide by immunofluorescence. We were not able to detect any propeptide immunoreactivity in the secretory granules stored in the cell tips, even though propeptide immunoreactivity was detected in the Golgi zone (data not shown). These data suggest that the propeptide epitope was not accessible in the acidic environment of the secretory granules, potentially because of interaction with the PC2 catalytic domain. The possibility that some of the propeptide was sorted out of the secretory granules into the lysosomes for degradation was not supported by studies of co-localization of the propeptide immunoreactive with LAMP-1, a lysosomal marker, even in the presence of lysosomal inhibitors.

Taken together, the experiments described above demonstrate that the PC2 propeptide fulfills the major functions of zymogen propeptides in the regulation of precursor activation. Such regulation is achieved at several levels as follows: 1) by directing the folding of the PC2 catalytic site; 2) by inhibiting PC2 activity; and 3) by terminating the inhibitory potency through endo- and exoproteolysis. Our data additionally indicate that internal cleavage of the propeptide is not a prerequi-

site for the activation of pro-PC2, as is the case for furin. We speculate that following primary site cleavage, insertion of the propeptide product containing the internal site into the catalytic pocket provides the structural switch that triggers release of the primary propeptide processing product, containing the inhibitory site, from the catalytic cleft. The relatively low affinity of PC2 propeptide fragments for PC2 (as compared with other convertase propeptide fragments for their propeptides) may constitute the reason that internal site insertion and cleavage is not required for activation of pro-PC2.

Acknowledgment—We are very grateful to J. Finley for expert assistance with cell culture.

REFERENCES

1. Rouille, Y., Duguay, S. J., Lund, K., Furuta, M., Gong, Q., Lipkind, G., Oliva, A. A. J., Chan, S. J., and Steiner, D. F. (1995) *Front. Neuroendocrinol.* **16,** 322–361
2. Seidah, N. G., and Chretien, M. (1997) *Curr. Opin. Biotechnol.* **8,** 602–607
3. Creemers, J. W., Jackson, R. S., and Hutton, J. C. (1998) *Semin. Cell Dev. Biol.* **9,** 3–10
4. Zhou, A., Webb, G., Zhu, X., and Steiner, D. F. (1999) *J. Biol. Chem.* **274,** 20745–20748
5. Gluschankof, P., and Fuller, R. S. (1994) *EMBO J.* **13,** 2280–2288
6. Zhou, A., Martin, S., Lipkind, G., LaMendola, J., and Steiner, D. F. (1998) *J. Biol. Chem.* **273,** 11107–11114
7. Molloy, S. S., Thomas, L., VanSlyke, J. K., Stenberg, P. E., and Thomas, G. (1994) *EMBO J.* **13,** 18–33
8. Creemers, J. W., Usac, E. F., Bright, N. A., Van de Loo, J. W., Jansen, E., Van de Ven, W. J., and Hutton, J. C. (1996) *J. Biol. Chem.* **271,** 25284–25291
9. De Bie, I., Marcinkiewicz, M., Malide, D., Lazure, C., Nakayama, K., Bendayan, M., and Seidah, N. G. (1996) *J. Cell Biol.* **135,** 1261–1275
10. Van de Loo, J. W., Creemers, J. W., Bright, N. A., Young, B. D., Roebroek, A. J., and Van de Ven, W. J. (1997) *J. Biol. Chem.* **272,** 27116–27123
11. Rehemtulla, A., Dorner, A. J., and Kaufman, R. J. (1992) *Proc. Natl. Acad. Sci. U. S. A.* **89,** 8235–8239
12. Creemers, J. W., Vey, M., Schafer, W., Ayoubi, T. A., Roebroek, A. J., Klenk, H. D., Garten, W., and Van de Ven, W. J. (1995) *J. Biol. Chem.* **270,** 2695–2702
13. Wagner, I., van Dyck, L., Savel'ev, A. S., Neupert, W., and Langer, T. (1997) *EMBO J.* **16,** 7317–7325
14. Valls, L. A., Hunter, C. P., Rothman, J. H., and Stevens, T. H. (1987) *Cell* **48,** 887–897
15. Klionsky, D. J., Banta, L. M., and Emr, S. D. (1988) *Mol. Cell. Biol.* **8,** 2105–2116
16. McIntyre, G. F., Godbold, G. D., and Erickson, A. H. (1994) *J. Biol. Chem.* **269,** 567–572
17. Sevarino, K. A., Stork, P., Ventimiglia, R., Mandel, G., and Goodman, R. H. (1989) *Cell* **57,** 11–19
18. Stoller, T. J., and Shields, D. (1989) *J. Cell Biol.* **108,** 1647–1655
19. Mach, L., Mort, J. S., and Glossl, J. (1994) *J. Biol. Chem.* **269,** 13036–13040
20. Gray, A. M., and Mason, A. J. (1990) *Science* **247,** 1328–1330
21. Suter, U., Heymach, J. V., Jr., and Shooter, E. M. (1991) *EMBO J.* **10,** 2395–2400
22. Khan, A. R., and James, M. N. (1998) *Protein Sci.* **7,** 815–836
23. Inouye, M. (1991) *Enzyme* (*Basel*) **45,** 314–321
24. Baker, D., Shiau, A. K., and Agard, D. A. (1993) *Curr. Opin. Cell Biol.* **5,** 966–970
25. Siezen, R. J., Leunissen, J. A. M., and Shinde, U. (95) in *Intramolecular Chaperones and Protein Folding* (Shinde, U., and Inouye, M., eds) pp. 233–256, R. G. Landes Co., Austin, TX
26. Shinde, U., and Inouye, M. (1995) *J. Mol. Biol.* **247,** 390–395
27. Lesage, G., Prat, A., Lacombe, J., Thomas, D. Y., Seidah, N. G., and Boileau, G. (2000) *Mol. Biol. Cell* **11,** 1947–1957
28. Boudreault, A., Gauthier, D., and Lazure, C. (1998) *J. Biol. Chem.* **273,** 31574–31580
29. Zhong, M., Munzer, J. S., Basak, A., Benjannet, S., Mowla, S. J., Decroly, E., Chretien, M., and Seidah, N. G. (1999) *J. Biol. Chem.* **274,** 33913–33920
30. Muller, L., and Lindberg, I. (1999) *Prog. Nucleic Acids Res. Mol. Biol.* **63,** 69–108
31. Guest, P. C., Arden, S. D., Bennett, D. L., Clark, A., Rutherford, N. G., and Hutton, J. C. (1992) *J. Biol. Chem.* **267,** 22401–22406
32. Benjannet, S., Rondeau, N., Paquet, L., Boudreault, A., Lazure, C., Chretien, M., and Seidah, N. G. (1993) *Biochem. J.* **294,** 735–743
33. Shen, F. S., Seidah, N. G., and Lindberg, I. (1993) *J. Biol. Chem.* **268,** 24910–24915
34. Zhou, A., and Mains, R. E. (1994) *J. Biol. Chem.* **269,** 17440–17447
35. Zhu, X., and Lindberg, I. (1995) *J. Cell Biol.* **129,** 1641–1650
36. Zhu, X., Muller, L., Mains, R. E., and Lindberg, I. (1998) *J. Biol. Chem.* **273,** 1158–1164
37. Westphal, C. H., Muller, L., Zhou, A., Zhu, X., Bonner-Weir, S., Schambelan, M., Steiner, D. F., Lindberg, I., and Leder, P. (1999) *Cell* **96,** 689–700
38. Lamango, N. S., Zhu, X., and Lindberg, I. (1996) *Arch. Biochem. Biophys.* **330,** 238–250
39. Elias, C. F., Saper, C. B., Maratos-Flier, E., Tritos, N. A., Lee, C., Kelly, J., Tatro, J. B., Hoffman, G. E., Ollmann, M. M., Barsh, G. S., Sakurai, T., Yanagisawa, M., and Elmquist, J. K. (1998) *J. Comp. Neurol.* **402,** 442–459
40. Zhu, X., Rouille, Y., Lamango, N. S., Steiner, D. F., and Lindberg, I. (1996) *Proc. Natl. Acad. Sci. U. S. A.* **93,** 4919–4924
41. Muller, L., Zhu, X., and Lindberg, I. (1997) *J. Cell Biol.* **139,** 625–638
42. Johanning, K., Juliano, M. A., Juliano, L., Lazure, C., Lamango, N. S., Steiner, D. F., and Lindberg, I. (1998) *J. Biol. Chem.* **273,** 22672–22680
43. Lindberg, I., van den Hurk, W. H., Bui, C., and Batie, C. J. (1995) *Biochemistry* **34,** 5486–5493
44. Williams, J. W., and Morrison, J. F. (1979) *Methods Enzymol.* **63,** 437–467
45. Furuta, M., Yano, H., Zhou, A., Rouille, Y., Holst, J. J., Carroll, R., Ravazzola, M., Orci, L., Furuta, H., and Steiner, D. F. (1997) *Proc. Natl. Acad. Sci. U. S. A.* **94,** 6646–6651
46. Lindberg, I. (1986) *J. Biol. Chem.* **261,** 16317–16322
47. Lamango, N. S., Apletalina, E., Liu, J., and Lindberg, I. (1999) *Arch. Biochem. Biophys.* **362,** 275–282
48. Zhou, A., Paquet, L., and Mains, R. E. (1995) *J. Biol. Chem.* **270,** 21509–21516
49. Taylor, N. A., Shennan, K. I., Cutler, D. F., and Docherty, K. (1997) *Biochem. J.* **321,** 367–373
50. Li, Y., and Inouye, M. (1994) *J. Biol. Chem.* **269,** 4169–4174
51. Creemers, J. W., Siezen, R. J., Roebroek, A. J., Ayoubi, T. A., Huylebroeck, D., and Van de Ven, W. J. (1993) *J. Biol. Chem.* **268,** 21826–21834
52. Matthews, G., Shennan, K. I., Seal, A. J., Taylor, N. A., Colman, A., and Docherty, K. (1994) *J. Biol. Chem.* **269,** 588–592
53. Zhou, A., Bloomquist, B. T., and Mains, R. E. (1993) *J. Biol. Chem.* **268,** 1763–1769
54. Coll, M., Guasch, A., Aviles, F. X., and Huber, R. (1991) *EMBO J.* **10,** 1–9
55. Cygler, M., Sivaraman, J., Grochulski, P., Coulombe, R., Storer, A. C., and Mort, J. S. (1996) *Structure* **4,** 405–416
56. James, M. N., and Sielecki, A. R. (1986) *Nature* **319,** 33–38
57. Gallagher, T., Gilliland, G., Wang, L., and Bryan, P. (1995) *Structure* **3,** 907–914
58. Shinde, U. P., Liu, J. J., and Inouye, M. (1997) *Nature* **389,** 520–522
59. Leduc, R., Molloy, S. S., Thorne, B. A., and Thomas, G. (1992) *J. Biol. Chem.* **267,** 14304–14308
60. Li, Y., and Inouye, M. (1996) *J. Mol. Biol.* **262,** 591–594
61. Volkov, A., and Jordan, F. (1996) *J. Mol. Biol.* **262,** 595–599
62. Menard, R., Carmona, E., Takebe, S., Dufour, E., Plouffe, C., Mason, P., and Mort, J. S. (1998) *J. Biol. Chem.* **273,** 4478–4484
63. Hu, Z., Haghjoo, K., and Jordan, F. (1996) *J. Biol. Chem.* **271,** 3375–3384
64. Stack, M. S., Itoh, Y., Young, T. N., and Nagase, H. (1996) *Arch. Biochem. Biophys.* **333,** 163–169
65. Carmona, E., Dufour, E., Plouffe, C., Takebe, S., Mason, P., Mort, J. S., and Menard, R. (1996) *Biochemistry* **35,** 8149–8157
66. Bhattacharjya, S., Xu, P., Zhong, M., Chretien, M., Seidah, N. G., and Ni, F. (2000) *Biochemistry* **39,** 2868–2877
67. Martens, G. J., Braks, J. A., Eib, D. W., Zhou, Y., and Lindberg, I. (1994) *Proc. Natl. Acad. Sci. U. S. A.* **91,** 5784–5787
68. Fricker, L. D., Evans, C. J., Esch, F. S., and Herbert, E. (1986) *Nature* **323,** 461–464
69. Shinole, U., Fu, X., and Inouye, M. (1999) *J. Biol. Chem.* **274,** 15615–15621